NREL/CP-520-25632

Electrical Characterization of Etched Grain-Boundary Properties from As-Processed px-CdTe Based Solar Cells

L.M. Woods and G.Y. Robinson
Colorado State University, Ft. Collins, CO

D.H. Levi
National Renewable Energy Laboratory

V. Kaydanov
Colorado School of Mines, Golden, CO

Presented at the National Center for Photovoltaics Program Review Meeting
Denver, Colorado
September 8-11, 1998

National Renewable Energy Laboratory
1617 Cole Boulevard
Golden, Colorado 80401-3393
A national laboratory of the U.S. Department of Energy
Managed by Midwest Research Institute
for the U.S. Department of Energy
under contract No. DE-AC36-83CH10093

Work performed under task number PV903101

October 1998

NOTICE

Available to DOE and DOE contractors from:
Office of Scientific and Technical Information (OSTI)
P.O. Box 62
Oak Ridge, TN 37831
Prices available by calling (423) 576-8401

Available to the public from:
National Technical Information Service (NTIS)
U.S. Department of Commerce
5285 Port Royal Road
Springfield, VA 22161
(703) 605-6000 or (800) 553-6847
or
DOE Information Bridge
http://www.doe.gov/bridge/home.html


Printed on paper containing at least 50% wastepaper, including 20% postconsumer waste

Electrical Characterization of Etched Grain-Boundary Properties from As-Processed px-CdTe based Solar Cells

L.M. Woods,* D.H. Levi, V. Kaydanov,** G.Y. Robinson,* and R.K. Ahrenkiel

National Renewable Energy Laboratory, 1617 Cole Blvd., Golden, Colorado 80401, USA
**Colorado State University, Ft. Collins, Colorado 80523, USA*
***Colorado School of Mines, Golden, Colorado 80401, USA*

ABSTRACT: An ability to lift off or separate the thin-film polycrystalline CdTe from the CdS, without the use of chemical etches, has enabled direct electrical characterization of the *as-processed* CdTe near the CdTe/CdS heterointerface. We use this ability to understand how a back-contact, nitric-phosphoric (NP) etch affects the grain boundaries throughout the film. Quantitative determination of the grain-boundary barrier potentials and estimates of doping density near the grain perimeter are determined from theoretical fits to measurements of the current vs. temperature. Estimates of the bulk doping are determined from high-frequency resistivity measurements. Also, a variable doping density within the grains of non-etched material has been determined. These results allow a semi-quantitative grain-boundary band diagram to be drawn that should aid in determining more-accurate two-dimensional models for polycrystalline CdTe solar cells.

INTRODUCTION

Most polycrystalline CdTe-based solar cells have lateral grain sizes of the same order as the minority-carrier diffusion length, or about 1 μm. Thus, grain boundaries can dramatically influence the device performance (1,2). It has also been demonstrated that diffusion of impurities occurs up grain boundaries from adjacent films during growth and subsequent processing of a CdS/CdTe device (3-5). This fact, in addition to defect segregation, can greatly affect the electrical properties of the grain boundaries in the resultant CdTe film. Recently, a correlation was established between the back-contact nitric-phosphoric (NP) etch and the electrical junction, 7.5 microns away, in a photoluminescence study (6). Thus, it appeared that the NP etch was affecting the grain boundaries throughout the film. Herein, we will make use of an ability to separate the post-processed thin-film polycrystalline CdTe from the CdS, SnO_2, and glass substrate to understand how the NP etch affects the grain boundaries' properties.

We will present quantitative determination of the grain-boundary barrier potentials, estimates of the doping density near the outside of the grain, and estimates of the bulk doping. We also report how these quantities vary as a function of depth into the film. These properties are determined from measurements of DC current versus temperature and AC electrical conductivity. These findings should aid in determining more-accurate two-dimensional models of the polycrystalline devices, which will enable a better understanding of the device operation.

EXPERIMENTAL CONDITIONS

All samples described herein were processed at the National Renewable Energy Laboratory (NREL). The CdTe film is deposited by close-spaced sublimation (CSS) onto CdS, which is deposited by a chemical-bath solution. The substrate was a bilayer SnO_2-coated Corning 7059 glass. The as-grown CdTe film thickness is about 10 μm. The CdTe/CdS devices then receive a high-temperature $CdCl_2$ vapor treatment. After this, a 30-second NP etch (about 1% nitric acid, 70% phosphoric acid, and 29% water) dip is performed on some samples. All samples are then ion-beam-milled to a depth of about 250 nm, which removes the conducting Te-rich surface from the samples that were NP etched. Further milling is performed to achieve the total film thickness of 10, 7.5, 5.0, 3.5, and 2.0 μm, to systematically study the effects of the NP etch on the grain boundaries versus depth. The remaining CdTe film is lifted off from the device by using a technique similar to that of von Windheim et al. (7), but developed independently at NREL for CdTe on CdS. In this manner, smooth films of CdTe formerly in contact with CdS can be made as large as 1.5 cm in diameter. Several parallel strips of gold contacts are then applied by evaporation and the use of metal masks. The contacts are 11 mm long and are spaced 0.4 mm apart.

Electrical measurements were made using a two-probe method, a heated copper block, a thermocouple, and a temperature controller. A Keithley 485 picoammeter was used for the DC current measurement that was fully automated with computer control. The AC resistance was measured using HP 4274 and 4275 LCR meters, which together provided a 100-Hz to 10-MHz frequency range. An HP 6825 external power supply provided bias control. Contact resistance was determined to be negligible using a three-probe technique and a method of variable contact spacing.

BACKGROUND

Previously, it has been demonstrated that the grain-boundary resistance dominates the CdTe film in-plane DC resistivity (8). Thus, the DC resistivity indicates the relative grain-boundary barrier height. The primary deterrent for determining the absolute grain-boundary potentials is the lack of knowledge of the doping density in the vicinity of the grain boundaries due to defect segregation and impurity diffusion. In this study, the conduction mechanism over the grain boundary will be determined by analyzing the dependence of conductivity on

temperature. Values of barrier height, V_b, and doping density in the vicinity of the grain boundary, N_b, are then taken from the grain-boundary conduction model that best fit the current versus temperature dependence. Conduction models considered are a combined drift-diffusion and thermionic emission model developed by Crowell and Sze (9), and a thermally assisted tunneling model developed by Padovani and Stratton (10). Conduction models are discussed in more detail in reference (8). The fitting assumes a simplifying approximation of uniform doping in the grain-boundary depletion region, N_b, and an isotropic effective mass due to the cubic nature of the CdTe film (11). Fits are obtained using user-defined functions in Peakfit Software®. Values of the grain-boundary barrier height and doping in the vicinity of the grain boundary are parameters of the fit and are taken directly from the best fit to the data.

RESULTS AND DISCUSSION

An example of the best fit for each of the conduction models is shown in Fig. 1 for the non-etched sample. As can be seen from the figure, the thermally assisted tunneling model gives the best fit. The barrier height, as determined by the thermally assisted tunneling model, was 0.78 eV, and N_b was about $7x10^{17}$ cm^{-3}. For comparison, V_b as determined from thermionic emission was 0.62 eV, using the maximum value of N_b, which is artificially set to 10^{17} cm^{-3}. Conduction models using values of N_b greater than 10^{17} cm^{-3} must consider tunneling (12). The separation in energy between the Fermi level and valence band, E_{fv}, is thus approximately 0.08 eV, using the value of N_b from the thermally assisted tunneling fit and a nominal value of effective density of states of $1.3x10^{19}$ cm^{-3} (13). Similar good fits can be obtained for the NP-etched samples. In this case, the thermionic model fits almost as well as the thermally assisted tunneling model. For comparison, a V_b of 0.30 eV was obtained for the thermionic-only fit, using the maximum N_b value, and a value of 0.28 eV was found from the thermally assisted tunneling fit.

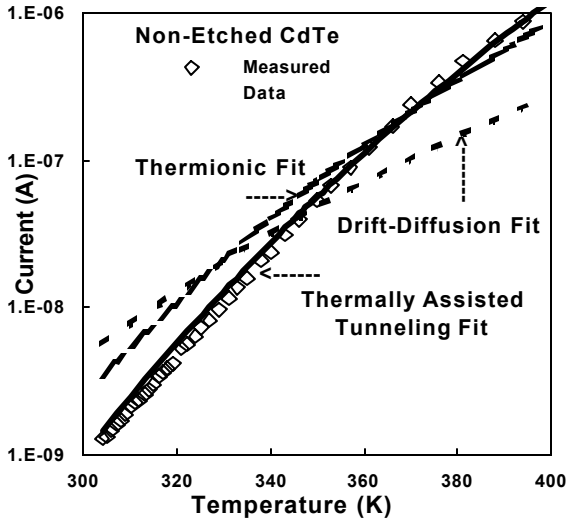

Figure 1. Comparison of theoretical fits to current vs. temperature data for different models of conduction.

To better understand the nature of grain-boundary changes due to the NP etch, grain boundary measurements were also performed under 1-sun illumination. During illumination, the barrier height of the NP-etched sample remained relatively unchanged, V_b = 0.23 eV, while the non-etched barrier height went to zero. This is an indication that a different material is

present in the grain boundaries after the NP etch and that this material then fixes the barrier height due to band offsets. It was shown previously that the NP etch preferentially etches grain boundaries and creates Te-rich grain boundaries (6). The value of $V_b + E_{fv} = 0.31$ eV (from the thermally assisted tunneling model) is approaching the value of 0.26 eV for the valence-band offset between evaporated Te and CdTe (14).

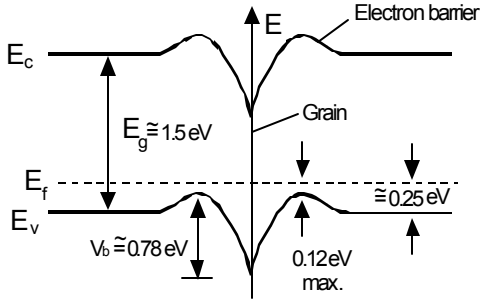

Figure 2. Grain-boundary band diagram of non-etched CdTe. V_b and N_b as determined from thermally assisted tunneling theory fit to current vs. temperature data.

The results of the fit and high-frequency resistance measurements for a non-etched sample allow us to calculate the shape of the band diagram in the dark, as seen in Fig. 2. The bulk doping level was estimated to be about $7x10^{14}$ cm^{-3} and was determined from the value of the high-frequency resistance, device geometry, and a nominal value of 60 cm^2/v-s as the bulk hole mobility in crystalline CdTe. This doping level is about three orders of magnitude less than the doping in the vicinity of the grain boundary and gives rise to a minimum minority-carrier barrier of about 0.13 eV near the potential barrier. The spatial extent of the highly doped region is unknown. However, the grain-boundary depletion region is about 0.1 μm, as determined from the Poisson's equation applied to a double depletion region, again assuming constant doping within the depletion region or $x_d = [(2\varepsilon_s V_b)/(qN_b)]^{1/2}$. Here, ε_s is the static dielectric constant for CdTe and q is the electronic charge.

Because it was shown that the NP etch reduces the grain-boundary barrier height, the next step was to determine the extent of this effect with depth in the sample. Fig. 3 plots V_b for each of the NP-etched samples that have been ion-beam-milled to various depths. Non-etched, but ion-beam-milled samples were also measured for comparison. Four samples were processed at each film thickness: two non-etched and two NP-etched. The bar thickness at every point indicates the variation between like samples. From this plot, we see that the NP etch losses its effects after 5 μm of film have been removed. It was later shown that an NP-etched material had a buried homojunction, as deduced from electron-beam-induced-current (EBIC) measurements, which occurs about 2.5 μm into the film, or thickness = 2.5 μm in Fig. 3. This would deplete the adjacent 1-2 μm, and thus, possibly affect the result up to a film thickness of 5 μm. The results below 5 μm are therefore poorly understood at this point. Measurements in the light were also performed (not shown). These measurements show differences in the illuminated barrier potentials up to and including the 5-μm film thickness, thus indicating that the effects of the NP etch extend down a minimum of 5 μm.

The 10-μm-thick samples that were lightly milled were periodically remeasured over 9 months to determine the stability of the barrier-reducing etch. The non-etched 10-μm samples were also remeasured for comparison, and the results are plotted in Figure 4. All samples were left in room atmosphere during this time. The different symbols

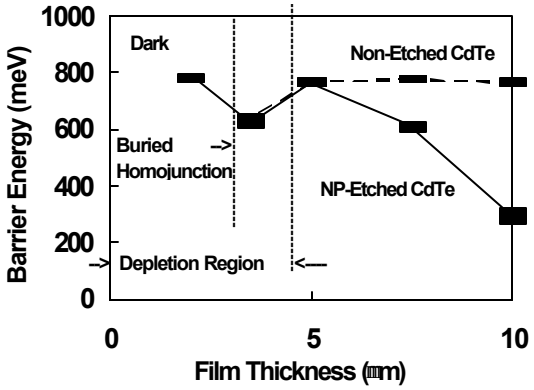

Figure 3. Effect of the NP etch on the CdTe grain-boundary barrier vs. depth. Possible extent of depletion region is shown due to buried homojunction.

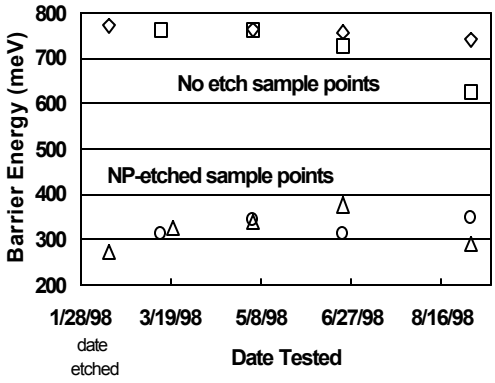

Figure 4. Grain boundary barrier height stability for 10 μm thick samples. Two NP-etched samples and two non-etched samples.

correspond to different samples. Looking at the first three points in time, it can be seen that the non-etched samples remained relatively stable, whereas the NP-etched samples degraded. This degradation is most likely due to oxidation of the tellurium in the grain boundaries. The oxidation of tellurium has been shown in a previous study using X-ray photoelectron spectroscopy (14). In that study, the $TeO_2/(Te+Te0_2)$ ratio went from about 0 to 0.3 in a matter of hours. Thus, it is likely that the NP-etched samples underwent a great deal of oxidation before the first samples were measured. However, the changes in the grain-boundary barrier height were still occurring even after several months. A change in the dark barrier height from 0.28 eV to 0.35 eV can increase the barrier resistance by an order of magnitude. This fact is important for devices relying on the NP etch to create a back-surface interface layer that is tellurium-rich to provide a low resistance back contact. The results of the figure indicate that although the barrier height appears to be stabilizing to a lower value than non-etched samples, some initial series-resistance increases can be expected.

CONCLUSIONS

Measurements of the NP-etched grain-boundary barrier heights correlate with trends from other measurements of valence-band offsets in a previous study. This previous study postulated that the NP etch reduced the barrier height by creating a p-type tellurium layer to compensate the n-type defects at the grain boundary (14). The effect of the NP etch on grain boundaries extends down a minimum of 5 μm. Also shown was a variable grain doping level in all samples, with increasing doping near the grain boundary of several orders of magnitude when compared to the bulk concentration. This information has allowed a detailed development of the grain-boundary band diagram, which predicts a minority-carrier or conduction-band barrier due to the variable doping. We postulate that if this layer is wider

than electron mean-free-path length, then this layer could act to reflect the minority carriers before the grain boundary, and thus, temper the grain-boundary barrier effects on minority-carrier recombination. Lifetimes measured by time-resolved photoluminescence and solar cell J_{sc} measurements (15) corroborate this and appear to be unchanged by the NP etch. Finally, it was shown that the effects of the NP etch are initially unstable and could result in severe increases in the back-contact series resistance of devices.

ACKNOWLEDGEMENTS

The authors would like to thank the following NREL employees: David Albin, for growing the samples; Yoxa Mahathongdy, for performing the $CdCl_2$ treatment; Anna Duda and Aaron Szalaj, for aiding in the metal evaporation; and Tim Gessert, for performing the ion-beam milling. This project was funded by the U.S. Department of Energy under Contract No. DE-AC36-83CH10093.

REFERENCES

1. Ahrenkiel, R.K., Keyes, B.M., Wang, L., and Albright, S.P., "Minority-Carrier Lifetime of Polycrystalline CdTe in CdS/CdTe Solar Cells," *Proceedings of the Twenty-Second IEEE PVSC*, 1991.
2. Lee, Y.J. and Gray, J.L., "Numerical Modeling of Polycrystalline CdTe and CIS Solar Cells," *Proceedings of the Twenty-Third IEEE PVSC*, 1993.
3. Levi, D.H., Woods, L.M., Albin, D.S., Gessert, T.A., Reedy, R.C., and Ahrenkiel, R.K., "The Influence of Grain Boundary Diffusion on the Electro-Optical Properties of CdTe/CdS Solar Cells," *Proceedings of the 2nd WCPVSEC/Twenty-Seventh IEEE PVSC*, 1998.
4. Annual Report, NREL Subcontract XAV-3-13170-01, pp. 75-85, 1994.
5. Dhere, R.G., Albin, D.S., Rose, D.H., Asher, S.E., Jones, K.M., Al-Jassim, M.M., Moutinho, H.R., and Sheldon, P., "Intermixing at the CdS/CdTe Interface and Its Effect on Device Performance," *Proceedings of the Materials Research Society Symposium,* Vol. 426, 1996.
6. Levi, D.H., Woods, L.M., Albin, D.S., Niles, D.W., Swartzlander, A., Rose, D.H., Ahrenkiel, R.K., and Sheldon, P., "Back Contact Effects on Junction Photoluminescence in CdTe/CdS Solar Cells," *Proceedings of the Twenty-Sixth IEEE PVSC,* 1997.
7. von Windheim, J., Renaud, I., and Cocivera, M., *J. Appl. Phys.,* **67**(9), (1990).
8. Woods, L.M., Levi, D.H., Kaydanov, V., Robinson, G.Y., and Ahrenkiel, R.K., "Electrical Characterization of CdTe Grain-Boundary Properties from As-Processed CdTe/CdS Solar Cells," *Proceedings of the 2nd WCPVSEC/Twenty-Seventh IEEE PVSC*, 1998.
9. Crowell, C.R. and Sze, S.M., *Solid-St. Electron*., **9**, p. 1035, (1966).
10. Padovani, F.A. and Stratton, R., *Solid-St. Electron*., **9**, p. 695, (1966).
11. Al-Jassim, M.M., private communication, 1998.
12. Fahrenbruch, A.L., and Bube, R.H., *Fundamentals of Solar Cells*, Academic Press, New York, N.Y., 1983, ch. 5, pp. 169, see Fig. 5.33.
13. Lee, Y.J., Gray, J.L., "Numerical Modeling of CdS/CdTe Solar Cells: A Parameter Study," *Proceedings of the Twenty-Second IEEE PVSC,* 1991.
14. Niles, D.W., Li, X., Sheldon, P., and Hochst, H., *J. of Appl. Phys*., **77**(9), p. 4489, (1995).
15. Li, X., private communication, 1997.